



Design, Synthesis, DFT Studies and Anticancer Activity of Novel Metal Complexes Containing 1,3,5-triazino[1,2-a]benzimidazole Moiety Using Microwave as an Approach for Green Chemistry



Ali M. Hassan¹, Bassem H. Heikal², Hamdy Khamis^{1,3}, Gamal Abd El-Naeem⁴, Emad Marzouk⁵, Miral A. Abdelmoaz⁶ and Ahmed Younis^{7*}

¹Chemistry Dep. Faculty of Science, Al-Azhar University, Nasr City 11884, Egypt.

²Research Laboratory, Cairo Oil Refining Company, Mostorod, Kaliobia, Egypt.

³Chemistry Dep. Faculty of Science and Arts, North Border University, Rafha, 91911, P.O. 840, Saudi Arabia.

⁴Polymer department, city of Scientific Research and Technology Applications, New Borg El-Arab Alexandria, Egypt.

⁵Researcher chemist, Pwt International Company, Alexandria, Egypt.

⁶Pharmaceutical Chemistry Department, Faculty of pharmacy, Sinai University.

⁷Green Chemistry Dept., National Research Centre, 33 El Bohouth St. (former EL Tahrir St.)-Dokki-Giza-Egypt.

2-(2-amino-4,10-dihydrobenzo[4,5]imidazo[1,2-a][1,3,5]triazin-4-yl)phenol (ligand) and its related metal complexes of Mn (II), Co (II), Ni (II), Cu (II) and Zn (II) were prepared under microwave irradiation. The structures of prepared compounds were elucidated in terms of elemental analysis, FT-IR, UV-Vis, ¹H NMR, ¹³C NMR, EPR spectra and mass spectra in addition to magnetic studies at room temperature and thermal properties. Elemental analysis results determined mole ratios between the ligand and metal 1:1 or 1:2. The microwave approach provides clean, shorter reaction times and enhancements in yields. Coats Redfern and Horowitz Metzger equation were used to study Thermal kinetic parameters of dehydration and decomposition of the complexes. The geometries of the ligand and its Mn (II), Co (II), Cu (II) and Zn (II) complexes were optimized using Gaussian 09 W; density functional theory (DFT) B3LYP method. Also, the cytotoxic activity of the ligand and its metal complexes were evaluated against liver cancer cells (HepG-2) and the Cu (II) complex exhibited the highest cytotoxic activity with promising IC₅₀ value = 3.5 μg/ml compared to standard reference cisplatin.

Keywords : Green chemistry, microwave, metal complexes, molecular modeling and anticancer activity.

Introduction

Cancer still one of the common reasons of death over our planet, although the great efforts were exerted to treat this disease, we need a new approach to improve the efficacy of current remedies against aggressive tumors. In recent decades, metal complexes are used in the development and design of anticancer where

metal complexes containing transition metals such as copper, nickel, cobalt and others can interact with active sites of enzymes via transition metal leading to increase its efficiency [1-3].

There is no doubt that benzimidazole compounds have a noticeable interest among chemists due to the wide spectrum of its applications [4-7] especially biological

*Corresponding author e-mail: younischem@gmail.com

Received 7/5/2020; Accepted 29/7/2020

DOI: 10.21608/ejchem.2020.29618.2639

© 2021 National Information and Documentation Center (NIDOC)

applications where many benzimidazole derivatives have antiviral [8], antibacterial [9, 10], antifungal [11,12], antihistaminic [13-15] or anticonvulsant activity [16,17]. In addition to the previously mentioned applications, benzimidazole derivatives exhibit good anticancer activity against different types of cancer [18-21]. Such as, Bendamustine (Trade Names Treanda®, Bendekalm, 1) is used for treatment of chronic lymphocytic leukemia (CLL) [22], Dovitinib (2) exhibits activity toward multiple RTK enzymes such as PDGFR and VEGFR [23, 24]. where it is applied for cases of gastrointestinal stromal tumor resistant to imatinib [25], Carbendazim (FB 642, 3) has anticancer activity in preclinical

trials, against colon cancer cell lines (HT-29) [26, 27]. Nocodazole (NSC-238189, 4) inhibits several kinases such as C-KIT, AB1 and MET so it has promised activity against many cancer cells [28] (Fig. 1).

Many 1,3,5-triazines derivatives were synthesized and exhibited inhibitory activities against various cell lines such as Altretamine (1,3,5-triazine derivative drug, 5) that is used in treatment of ovarian cancer [29-31], also a variety of substituted 1,3,5-triazine derivatives were studied and displayed anticancer activity such as ZSTK474 compound 6 and AMG 511 compound 7 [32, 33] (Fig. 2).

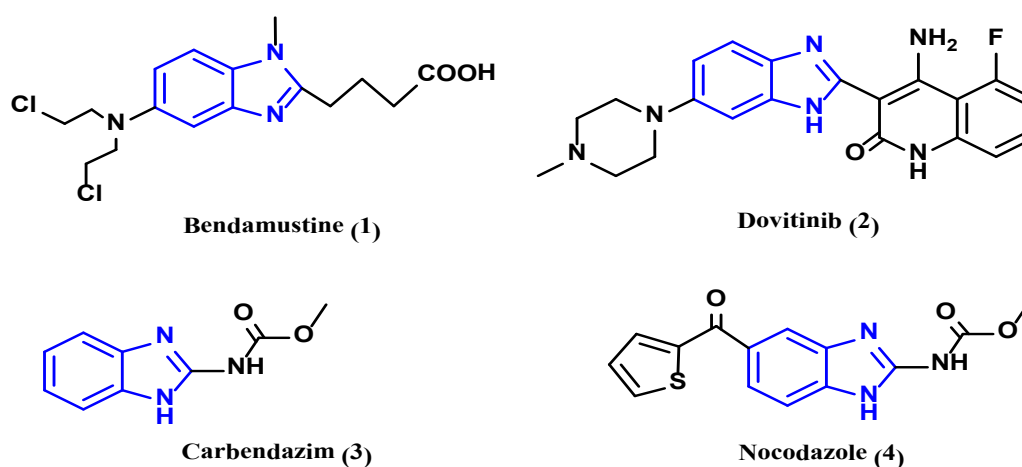


Fig. 1. Reported benzimidazole anticancer agents.

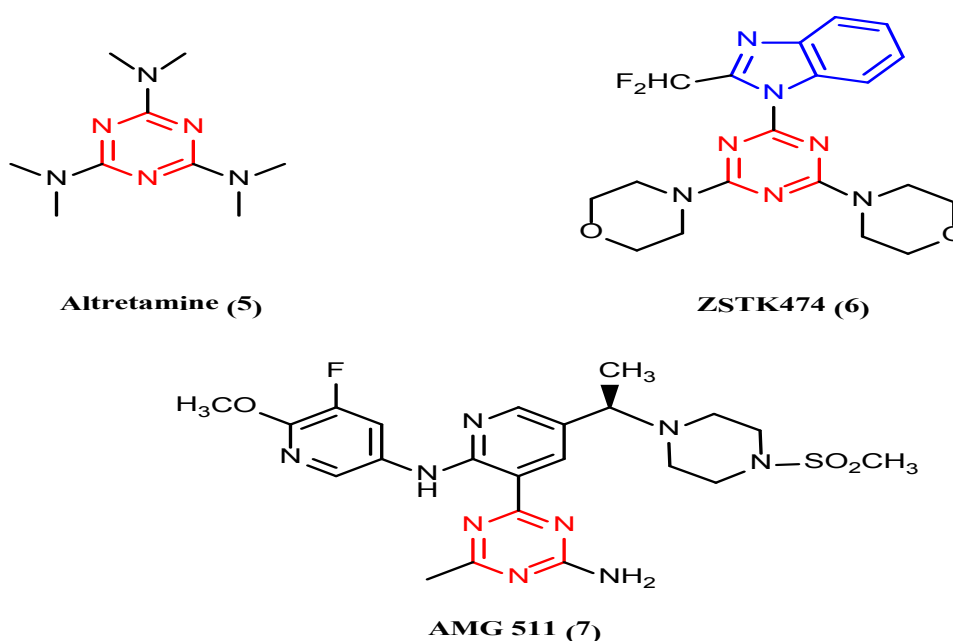


Fig. 2. Reported 1,3,5-triazine anticancer agents.

In continuation of our interest in green chemistry and synthesis [34-44], we aim to use microwave irradiation for synthesis of novel zinc, copper, nickel, cobalt and manganese complexes based on 1,3,5-triazino [1,2-a] benzimidazole moiety and studying the effect of metal on the biological activity of ligand where the antitumor activity of ligand and its metal complexes against HepG2 were studied and compared.

Experimental

Materials and physical measurements

All organic solvents were purchased from commercial sources and used as received or dried using standard procedures unless otherwise stated. All chemicals were purchased from Merck, Aldrich and used without further purification, thin layer chromatography (TLC) was performed on precoated Merck 60 GF 254 silica gel plates with fluorescent indicator, detection by means of UV light at 254 and 360 nm. Melting point was measured by electrothermal apparatus, without correction. The UV-Vis range (9091-52631 cm^{-1}) using Jenway 6715 UV/Vis spectrophotometer at holding company for water and wastewater, all of compounds dissolved in glacial acetic acid before measurements. The Fourier transform infrared spectra of the ligand, as well as the metal complexes using KBr, were recorded on Vertex 70 Analyzer, Bruker, USA from 4000–400 cm^{-1} and metal ions estimation was determined by complexometric titration using general lab glassware [45] at the faculty of science, Al-Azhar University, Cairo, Egypt. The magnetic susceptibility of the solid complexes was carried out at room temperature by the Gouy's technique for magnetic susceptibility instrument.

The thermogravimetric analyses (TGA) of the solid complexes were performed using the Shimadzu TG-50 thermogravimetric analyzer with a heating rate of 10°C/min under nitrogen atmosphere, in the range of 25–800°C at the faculty of sciences, Cairo University. The thermodynamic activation parameters of decomposition processes of dehydrated complexes namely activation energy (E^*), enthalpy (ΔH^*), entropy (ΔS^*) and Gibbs free energy change of the decomposition (ΔG^*) are evaluated graphically by employing the Coats–Redfern [46] relation and Horowitz-Metzger [47]. The thermodynamic activation parameters for the thermal decomposition steps in complexes were calculated using the relationships:

$$\Delta H = E^* - RT \quad (1)$$

$$\Delta S^* = R[\ln(Ah/kT) - 1] \quad (2)$$

$$\Delta G^* = \Delta H^* - T\Delta S^* \quad (3)$$

Where R is the universal gas constant, A is the frequency factor, h is Planck's constant and k is Boltzmann constant.

The ESR spectra of the powdered Cu(II) sample were carried out on Bruker-EMX-(Xbands-9.7 GHz) spectrometer with 100 KHz frequency, microwave power 1.008 MW, modulation/amplitude of 4 GAUSSES at National Center for Radiation Research and Technology, Egyptian Atomic Energy Authority. The elemental analysis for carbon, hydrogen and nitrogen are carried out using a Flash 2000 organic Elemental Analyzer, Thermo, USA, the mass spectra were performed by Shimadzu Qp-2010 plus by GCms Solution. The cytotoxicity evaluation was applied against one cell line; liver cancer cells (HepG-2) inhibitory activity against Hepatocellular carcinoma cell, read the absorbance at 490 nm using ELISA reader (SunRise, TECAN, INC, USA) were studied at the Regional Center for Mycology & Biotechnology Al-Azhar University. The ^1H NMR and ^{13}C spectra were recorded on an Agilent Technologies model spectrometer NMR400-mercury. ^1H spectra were run at 300 MHz and ^{13}C spectra were run at 75.46 MHz in dimethylsulphoxide (DMSO- d_6). Tetramethylsilane (TMS) was used as an internal reference and chemical shifts are quoted in δ (ppm) at the Main Chemical Warfare Laboratories, Chemical Warfare Department, Ministry of Defense, Cairo, Egypt. Microwave-assisted reactions conducted on a commercially household microwave energy output 900 W, frequency 2450 MHz, manufactured by DAEWOO technologies Corporation, model: KOR-9G2B, Korai.

Synthesis and preparation

synthesis of 2-guanidinobenzimidazole (2-GB)

A mixture of o-phenylenediamine (1 mol.), dicyandiamide (1 mol.), concentrated hydrochloric acid (2 moles) and distilled water was heated under reflux for 3 hours. The reaction mixture allowed to cool down and treated with 10% NaOH to afford the crude products 2-GB (Scheme 1) [48]. The solid product in the present study has been recrystallized from methanol to afford pure needles in 67% yield.

Synthesis of 2-(2-amino-4,10-dihydrobenzo [4,5]imidazo[1,2-a][1,3,5]triazin-4-yl)phenol (ligand)

An equimolar amount (1:1) ratio of 2-guanidinobenzimidazole and salicylaldehyde was refluxed and stirred for 5 hours in the presence of piperidine as catalyst (Scheme 1). The progress of the reaction and purity of the product was monitored by TLC. The product was recrystallized with hot methanol to afford 2-(2-amino-4,10-dihydrobenzo [4,5]imidazo [1,2-a] [1,3,5]triazin-4-yl)phenol in excellent yield (92.66%).

Preparation of the solid complexes

All the isolated solid complexes were prepared by mixing equimolar amounts of the prepared ligand and metal (II) acetates [M = Mn (II), Co(II), Ni(II), Cu(II), and Zn(II)] in presence of 4-6 drops of methanol as solvent. The reaction mixtures were subjected to microwave for appropriate time (4-6 min.) to afford metal complexes in good yields (73-87 %). The obtained products were washed by hot methanol and ether then finally dried under reduced pressure over anhydrous CaCl₂ in a desiccator (Scheme 2). The progress of the reaction and purity of the products were monitored by TLC. Table 1 shows the elemental analysis and physical properties of the amine, novel ligand and their metal complexes.

Molecular Modelling Methodology

The optimized structural geometries of ligand and its Mn (II), Co (II), Cu (II) and Zn

(II) complexes were determined using the DFT/B3LYP method with different basis sets using Gaussian 09 software [49]. Gauss-View molecular visualization program was used to display Gaussian files. [50] In agreement with the numerical pattern appearing in the view of the compounds in gas phase, significant bond lengths and angles in optimized structures were deduced.

Ni (II) complex was not implemented in Gaussian 09 software because our computer cannot perform it.

Cytotoxicity evaluation using viability assay

The cells were seeded in 96-well plate at a cell concentration of 1×10^4 cells per well in 100 μ l of growth medium. Fresh medium containing different concentrations of the test sample was added after 24 h of seeding. Serial two-fold dilutions of the tested chemical compound were added to confluent cell monolayers dispensed into 96-well, flat-bottomed microtiter plates (Falcon, NJ, USA) using a multichannel pipette. The microtiter plates were incubated at 37°C in a humidified incubator with 5% CO₂ for a period of 24 h. Three wells were used for each concentration of the test sample. Control cells were incubated without test sample and with or without DMSO. The little percentage of DMSO present in the wells (maximal 0.1%) was found not to affect the experiment. After incubation of the cells for at 37°C, for 24 h, the viable cells yield was determined by a colorimetric method [51].

TABLE 1. Melting points, yields, reaction time, analytical and physical properties of the prepared compounds.

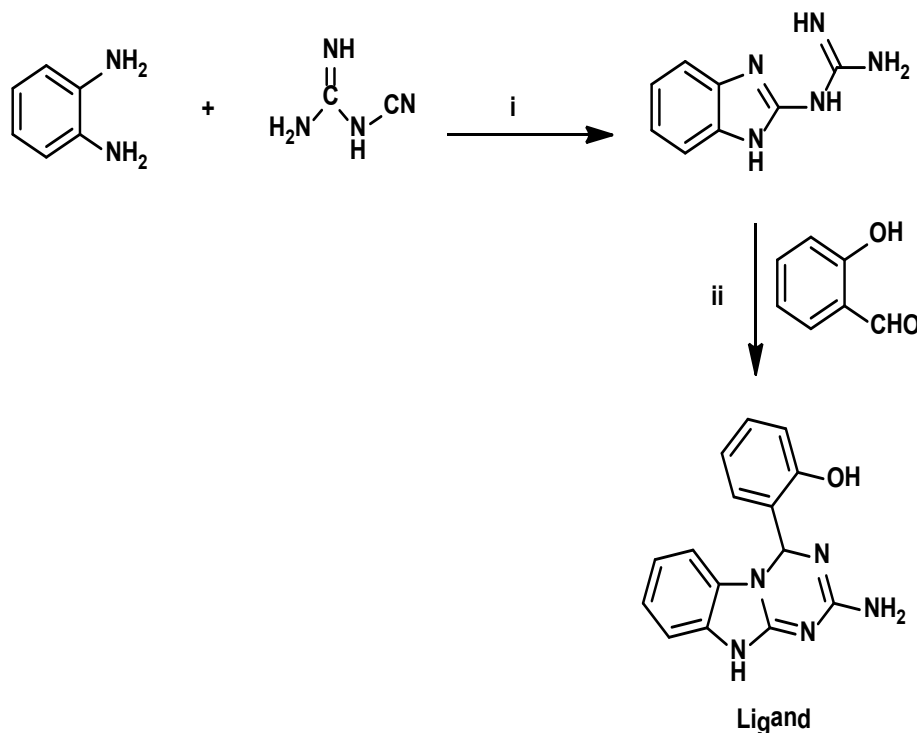
Comp.	Molecular Formula	M.P °C	Yield %	Time min	Color	Elemental Analysis				M ⁺ Calc./ (Found)
						C	H	N	M	
Start	C ₈ H ₉ N ₅	242	67	180	Buff crystal	54.85 (54.73)	5.18 (5.14)	39.98 (40.1)	-	175.20 (175)
Ligand	C ₁₅ H ₁₃ N ₅ O	272	92.66	180	White	64.51 (64.24)	4.69 (5.18)	25.07 (25.29)	-	279.30 (279.11)
Mn	C ₁₇ H ₂₁ MnN ₅ O ₆	>330	76.8	4	Buff	45.75 (45.32)	4.74 (4.51)	15.69 (15.09)	12.31 (11.57)	446.09 (446)
Co	C ₁₇ H ₁₇ CoN ₅ O ₄	>330	85.6	5	Dark Green	49.29 (49.19)	4.14 (4.06)	16.9 (16.77)	14.23 (14.10)	414.28 (414)
Ni	C ₃₁ H _{31.5} N ₁₀ NiO ₆	>330	73.77	5	Reddish orange	53.2 (52.83)	4.65 (4.60)	20.04 (19.97)	10.93 (11.78)	698.5 (699)
Cu	C ₁₇ H ₁₉ CuN ₅ O ₅	>330	75.22	5	Black	46.73 (46.37)	4.38 (3.92)	16.03 (15.60)	14.54 (14.61)	436.07 (436)
Zn	C ₁₇ H ₁₇ N ₅ O ₄ Zn	>330	87.7	6	Pale Yellow	48.53 (48.32)	4.07 (4.45)	16.65 (16.22)	15.54 (14.87)	419.06 (419)

In brief, after the end of the incubation period, media were aspirated and the crystal violet solution (1%) was added to each well for at least 30 minutes. The stain was removed and the plates were rinsed using tap water until all excess stain is removed. Glacial acetic acid (30%) was then added to all wells and mixed thoroughly, and then the absorbance of the plates were measured after gently shaken on Microplate reader (TECAN, Inc.), using a test wavelength of 490 nm. All results were corrected for background absorbance detected in wells without added stain. Treated samples were compared with the cell control in the absence of the tested compounds. All experiments were carried out in triplicate. The cell cytotoxic effect of each tested compound was calculated. The optical density was measured with the microplate reader (SunRise, TECAN, Inc, USA) to determine the number of viable cells and the percentage of viability was calculated as $[(OD_t/OD_c)] \times 100\%$ where OD_t is the mean optical density of wells treated with the tested sample and OD_c is the mean optical density of untreated cells. The relation between surviving cells and

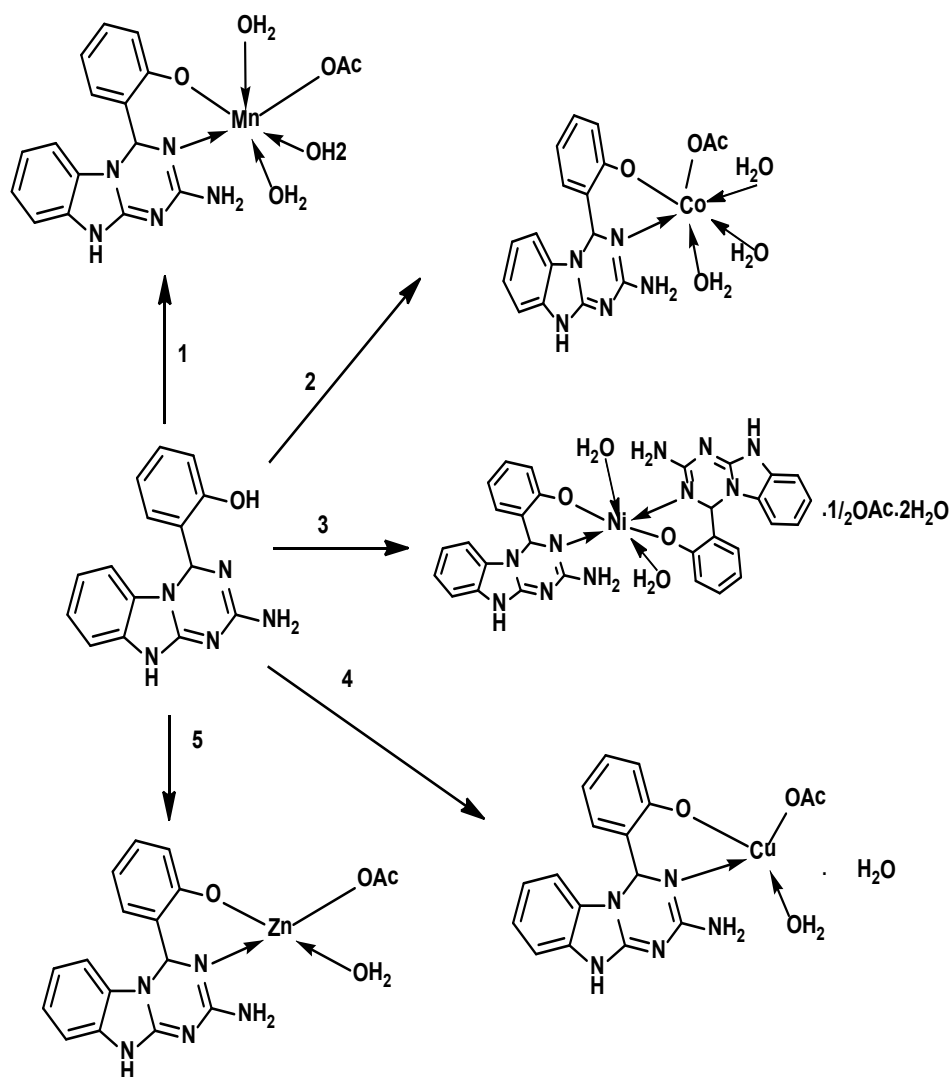
drug concentration is plotted to get the survival curve of each tumor cell line after treatment with the specified compound. The 50% inhibitory concentration (IC_{50}), the concentration required to cause toxic effects in 50% of intact cells, was estimated from graphic plots of the dose response curve for each conc. using Graph pad Prism software (San Diego, CA, USA).

Results and Discussion

The ligand 2-(2-amino-4,10-dihydrobenzo [4,5] imidazo [1,2-a] [1,3,5] triazin-4-yl) phenol was prepared by the reaction of 2-guanidinobenzimidazole and salicylaldehyde (Scheme 1). Then reacted with metal (II) acetates under microwave irradiation as an approach for green chemistry (Scheme 2) all structures were confirmed based on the elemental analysis and spectroscopic data. All compounds containing six member rings with -N- heterocycle and oxygen atom possess basic characteristics due to the presence of lone pair electron-donating character of the double bond of (-C=N) and the capability to form metal complexes as illustrated in Scheme (2).



Scheme 1. (i) reflux 3h, 2 moles HCl; (ii) reflux 5h, piperidine.



Scheme 2. 1) Manganese acetate tetrahydrate, 2) Cobalt acetate tetrahydrate, 3) Nickel acetate tetrahydrate, 4) Copper acetate monohydrate, 5) Zinc acetate dihydrate.

IR spectra

The IR spectra of 2-guanidinobenzimidazole revealed characteristic bands at 3444-3425, 3187 and 1651 cm^{-1} due to (NH_2), (N-H) and ($\text{C}=\text{N}$) respectively, while in the IR spectra of 2-(2-amino-4,10-dihydrobenzo[4,5]imidazo[1,2-a][1,3,5]triazin-4-yl) phenol (ligand) four characteristic bands appeared at 3534, 3437-3410, 3132 and 1616 cm^{-1} due to (OH), (NH_2), (N-H) and ($\text{C}=\text{N}$) respectively in addition to bands at 2954 and 3055 due to aliphatic and aromatic (C-H) (Table 2)_ENREF_21.

In metal complexes, 2-(2-amino-4,10-dihydrobenzo[4,5]imidazo[1,2-a][1,3,5]triazin-4-yl) phenol coordinate with the metal ions in di-dentate forming stable six-membered chelate

rings around the metal ions. this diverse behavior of ligand can be confirmed by comparing IR bands of complexes with IR bands of ligand as following :

1. The ($\text{C}=\text{N}$) stretch shows either a negative or positive shift on complexation [52, 53].
2. Vibration of $\nu(\text{M}-\text{N})$ in all the metals (II) complexes, exhibited a new band 537-439 cm^{-1} proving the coordination of nitrogen of azomethine with the metal ions and these within the band of 411-458 cm^{-1} are assigned to $\nu(\text{M}-\text{O})$ [54].
3. All other bands of ligand and their corresponding metal complexes appeared at the same region without change.

TABLE 2. Shows the main IR bands displayed by 2-guanidinobenzimidazole, ligand and novel complexes.

Sym.	$\nu(\text{OH}),$ H_2O	$\nu(\text{NH}_2)$	$\nu(\text{NH})$	$\nu(\text{C-H})$ Ar/Alph	$\nu(\text{C=N})$	$\nu(\text{C=C})$	$\nu(\text{C-O})$	$\nu(\text{OAc})$	$\nu(\text{M-N})$	$\nu(\text{M-O})$
2-GB	-	3444 3425	3187	3101 3055	1651	1508	-	-	-	-
Ligand	3534	3437 3410	3132	3055 2954	1616	1523	-	-	-	-
L-Mn	3589	3433 3409	3130	3056 2926	1619	1523	1352	1456	537	412
L-Co	3564	3441 3352	3217	3059 2927	1620	1519	1273	1458	505	439
L-Ni	3583	3406 3340	3136	3059 2931	1620	1519	1276	1462	474	435
L-Cu	3541	3425 3348	3218	3058 2925	1605	1519	1278	1457	529	458
L-Zn	3587	3416 3345	3138	3055 2929	1655	1525	1289	1449	439	411

Electronic spectra and magnetic properties

The electronic absorption spectra of the ligand and its complexes as shown in Table 3 were performed in glacial acetic acid. The electronic spectra of the ligand showed four absorption bands at 33112 cm^{-1} refers to $n \longrightarrow \pi^*$, of C=Nbenzimidazole and at 33783 cm^{-1} refers to $\pi \longrightarrow \pi^*$, of C = Nazomethane. The third band was at 39062 cm^{-1} refers to $\pi \longrightarrow \pi^*$, of C=C aromatic rings and band at 46296 cm^{-1} refers to $n \longrightarrow \sigma^*$, of phenolic group. For Mn (II) complex: The electronic spectra of Mn (II) complex showed absorption bands at (26315, 21052) cm^{-1} assigned to ${}^6\text{A}_{1g} \rightarrow {}^4\text{T}_{1g}$ (G) and ${}^6\text{A}_{1g} \rightarrow {}^2\text{T}_{2g}$ (G) transition respectively. The observation of these bands suggests an octahedral configuration around Mn (II) ion and the complex is paramagnetic where the magnetic moment is 4.18 BM. For Co (II) complex: The electronic spectra of Co (II) complex showed bands of appreciable intensity at (17857, 15625) cm^{-1} and assigned to ${}^4\text{T}_{1g} \rightarrow {}^4\text{A}_{2g}$ (F) and ${}^4\text{T}_{1g}$ (F) $\rightarrow {}^4\text{T}_{2g}$ (P) transitions respectively. The observation of these bands suggests an octahedral and the complex is paramagnetic and the magnetic moment is 5.14 BM. For Ni (II) complex: The electronic spectra of the Ni (II) showed absorption bands at

(21141, 19011) cm^{-1} assigned to ${}^3\text{A}_{2g} \rightarrow {}^3\text{T}_{1g}$ (P) and ${}^3\text{A}_{2g} \rightarrow {}^3\text{T}_{1g}$ (F) transition respectively. The observation of these bands suggests an octahedral configuration around Ni (II) and the magnetic moment is 2.25 B.M. For Cu (II) complex: The electronic spectra of the Cu(II) complex revealed bands of considerable intensity at (16393) cm^{-1} assigned to the transitions (${}^2\text{B}_{1g} \rightarrow {}^2\text{A}_{1g}$) assuming a tetrahedral configuration, thus the prepared Cu (II) are paramagnetic, the obtained magnetic moment value 1.38 B.M. For Zn(II) complex: the absorption bands at the range (21008) cm^{-1} for ligand in The electronic spectra of Zn (II) complex can be assigned to metal ligand (M \rightarrow L) transition and its position in agreement with low-spin tetrahedral geometry for Zn(II) complex and the complex is diamagnetic.

Mass spectra

The mass spectra chart of 2-guanidinobenzimidazole revealed molecular ion peak at $m/e = 175$ which is corresponding to its structure (figure 3). The molecular ion peak of the ligand and its nickel complex are showed at $m/e = 279$ and $m/e = 699$ respectively as shown in figures 4 and 5 which are corresponding to their structure.

TABLE 3. Magnetic, ESR and spectral data of the ligand and their metal complexes.

Comp.	λ_{\max} , cm ⁻¹	Assignments	μ_{eff} (BM)	g_{\square}	g^{\parallel}	g_{av}	Suggested Structure
Ligand	33112	(n- π^* , C=N),	-	-	-	-	-
	33783	(π - π^* , C=N),					
	39062	(π - π^* , aromatic ring)					
	46296	(n- σ^* , phenolic group)					
L-Mn	26315	${}^6A_{1g} \rightarrow {}^4T_{1g}$ (G)	4.18	-	-	-	Octahedral
	21052	${}^6A_{1g} \rightarrow {}^2T_{2g}$ (G)					
L-Co	17857	${}^4T_{1g}(\text{F}) \rightarrow {}^4A_{2g}$	5.14	-	-	-	Octahedral
	15625	${}^4T_{1g}(\text{F}) \rightarrow {}^4T_{2g}(\text{P})$					
L-Ni	21141	${}^3A_{2g} \rightarrow {}^3T_{1g}(\text{P})$	2.25	-	-	-	Octahedral
	19011	${}^3A_{2g} \rightarrow {}^3T_{1g}(\text{F})$					
L-Cu	16393	${}^2B_{1g} \rightarrow {}^2A_{1g}$	1.38	2.14	2.08	2.12	Tetrahedral
L-Zn	21008	M \rightarrow L	Dia	-	-	-	Tetrahedral

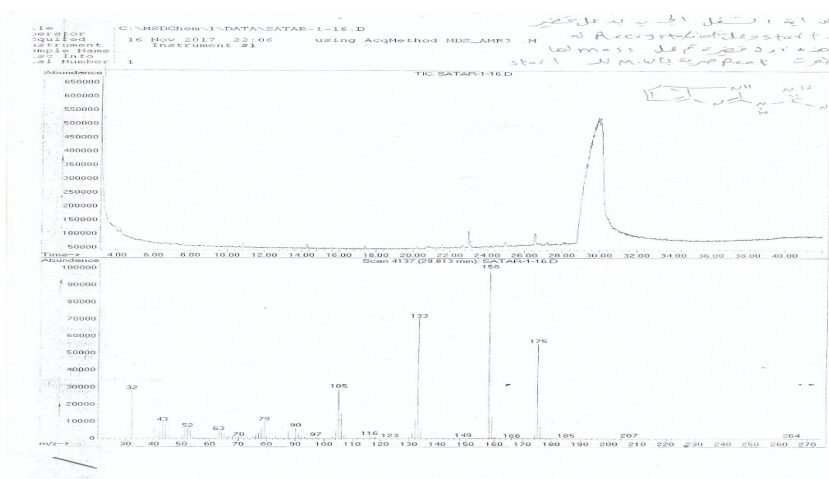


Fig. 3. Mass spectra of 2-guanidinobenzimidazole.

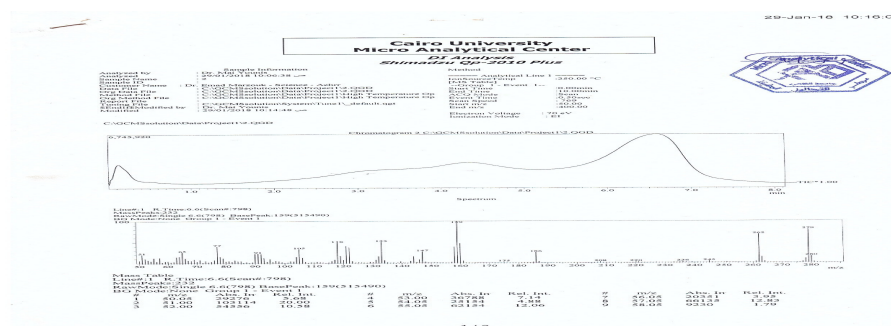


Fig. 4. Mass spectra of ligand.

NMR Spectra

The ^1H NMR spectra of ligand have been recorded in DMSO-d_6 . The ^1H NMR (DMSO) of ligand showed peaks at $\delta = 6.31$ ppm (s, 1H, NH), 6.69-7.1 ppm (m, 8H_{arom}), 7.25 ppm (s, 2H, NH_2), 7.72 ppm (s, 1H, triazino carbon (C15)) and 10.24 ppm (s, 1H, O-H) (Fig. 6). The ^{13}C NMR (DMSO) of the ligand showed peaks

at $\delta = 61.561$ ppm (C15), 108.26 ppm (C14), 116.23 ppm (C13), 116.27 ppm (C12), 119.25 ppm (C11), 119.66 ppm (C10), 121.11 ppm (C9), 126.38 ppm (C8), 127.02 ppm (C7), 130.46 ppm (C6), 131.88 ppm (C5), 143.69 ppm (C4), 154.32 ppm (C3), 155.03 ppm (C2) and 156.05 ppm (C1) (Fig. 7).

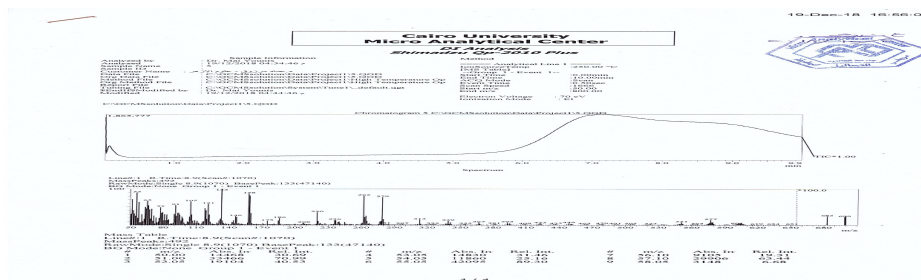


Fig. 5. Mass spectra of Ni (II) complex.

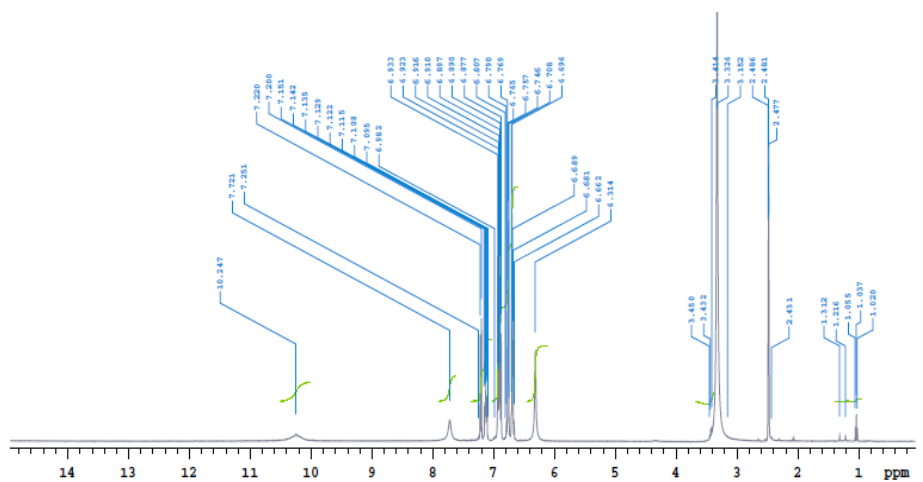


Fig. 6. ^1H NMR spectra of the ligand in DMSO-d_6 .

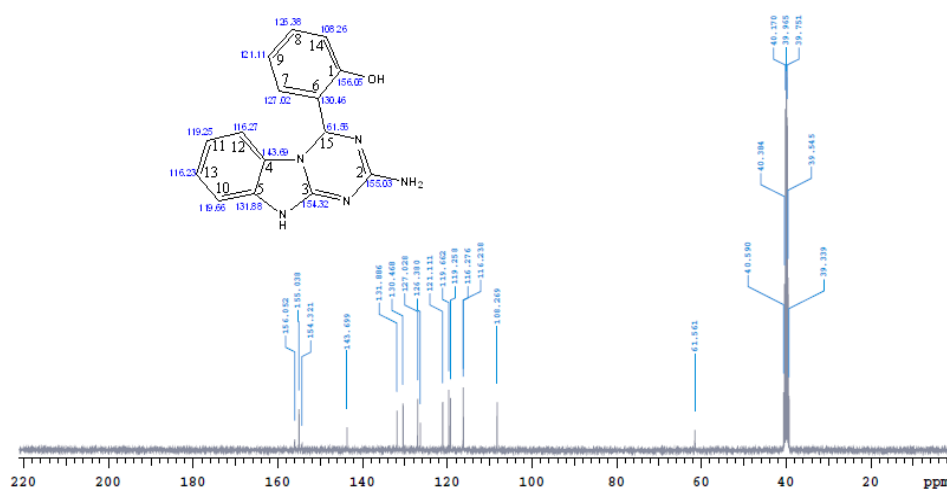


Fig. 7. ^{13}C NMR spectra of the ligand in DMSO-d_6 .

Electron spin resonance Spectrum (ESR)

The spectra of the complexes exhibit a single anisotropic broad signal with hyperstructure indicating the contribution of free acetate ligand with complex formation. The ESR spectra of the Ligand-Cu complex as shown in Table 3. It is showed broad signals with two "g" values (g_{\parallel} , g_{\perp}) (Fig. 8). For all complexes the value of g_{\parallel}

$< g_{\perp} < 2.3$ [55] suggesting covalent character of copper–ligand bonds in the present complex, where, $g_{\parallel} > 2.3$ concerns to ionic metal–ligand bond characteristic of complex with $2B_1(dx^2-y^2)$ orbital ground state. The average g values were calculated according to the equation $g_{av} = 1/3[g_{\parallel} + 2g_{\perp}]$ and it was equal to 2.12 for copper complex of ligand respectively [56].

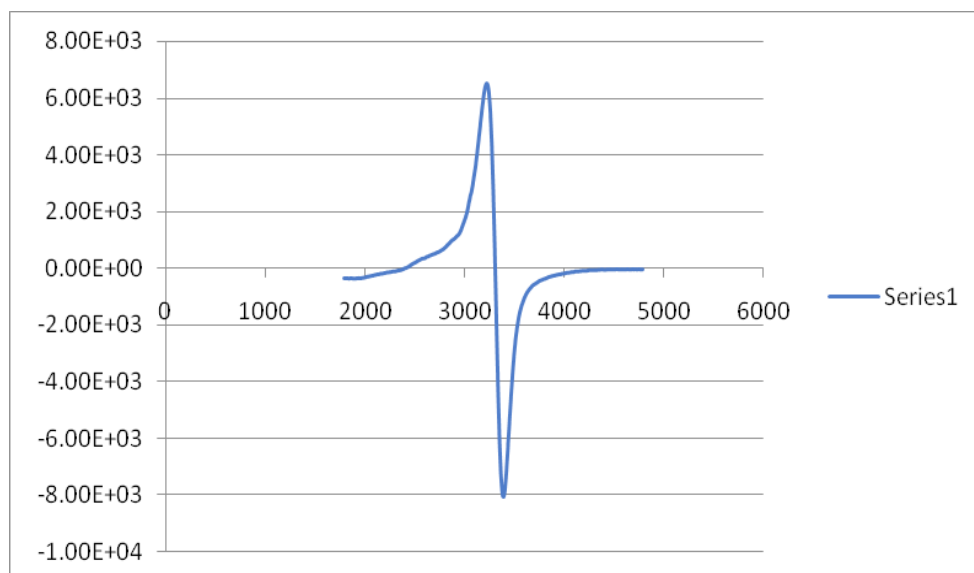
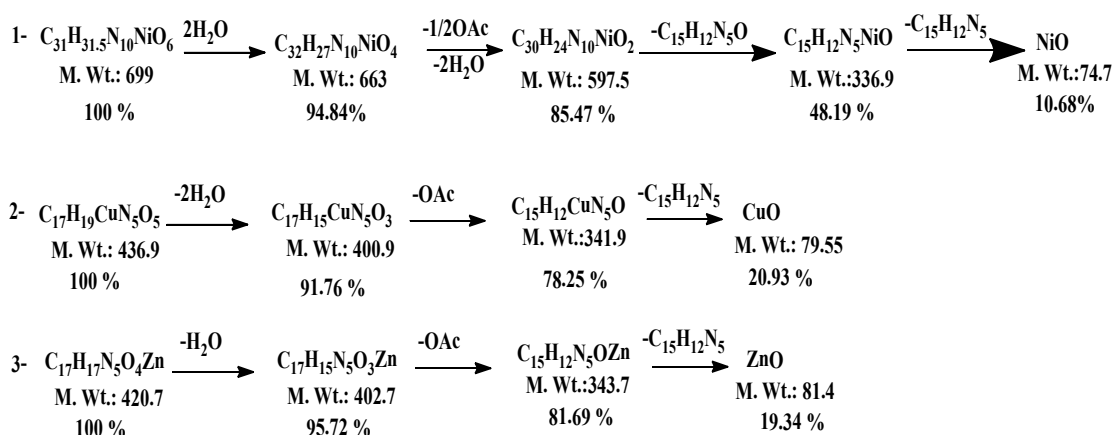


Fig. 8. ESR spectra of the Cu(II) complex.

Thermal analysis (TG)

The results of thermal gravimetric analysis of nickel (II), copper (II) and zinc (II) complexes

are showed in Table 4 and can be summarized as follow :



Thermo-kinetic parameters

Kinetic parameters of different stages were summarized in Table 5. From those results we concluded that :

1- The reactions are endothermic and most of

these reactions are slow and the reactants are less stable than products.

2- the values of ΔG increase which means that the reactions are non-spontaneous.

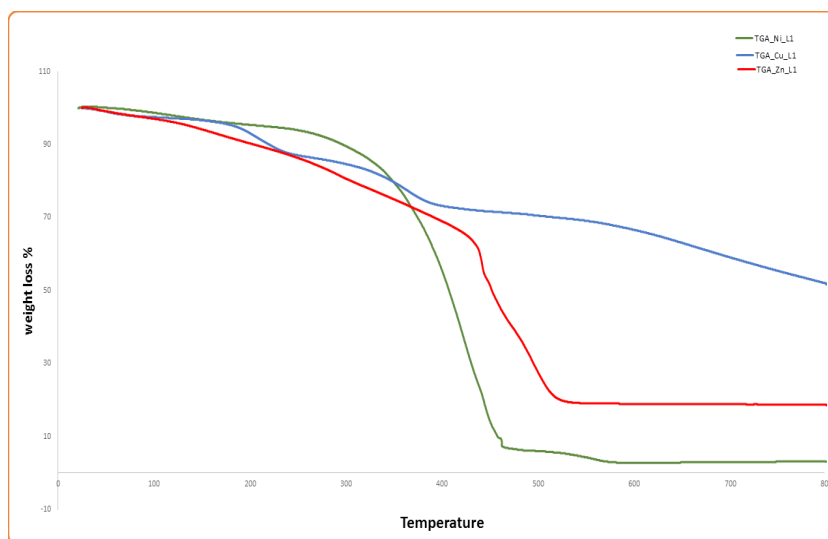


Fig. 9. Thermal analysis of nickel, copper(II) and zinc(II) complexes.

TABLE 4. Thermo-gravimetric data of the thermal decomposition of Ni (II), Cu (II) and Zn (II) complexes.

Ligand	Complex	Molecular Formula	Molecular Weight	Steps	ΔT °C		mass %		Assignment
					T_i	T_f	Calc.	Found	
L	Ni	$C_{31}H_{31.5}N_{10}NiO_6$	699	1 st	22	157	5.15	5.63	$2H_2O$
				2 nd	180	320	14.5	14.02	$2H_2O, 1/2OAc$
				3 rd	340	526	51.8	52.3	$C_{15}H_{12}N_5$
				4 th	560	700	37.48	37.3	$C_{15}H_{12}N_5$
					Residue			10.68	NiO
	Cu	$C_{17}H_{19}CuN_5O_5$	436.9	1 st	40	152	8.24	7.69	$2H_2O$
				2 nd	240	390	13.51	12.92	AcO
				3 rd	410	555	57.32	56.67	$C_{15}H_{12}N_5$
				Residue				18.20	CuO
	Zn	$C_{17}H_{17}N_5O_4Zn$	420.7	1 st	24	126	4.28	4.23	H_2O
				2 nd	240	414	14.03	14.13	AcO
				3 rd	405	575	62.35	62.23	$C_{15}H_{12}N_5$
Residue							19.34	ZnO	

TABLE 5. Thermodynamic data of the thermal decomposition of Ni(II), Cu(II) and Zn(II) complexes of ligand.

Complexes	Steps	Coats Redfern						Horowitz-Metzger					
		R^2	Ea KJ mol ⁻¹	A S ⁻¹	ΔS^* mol ⁻¹ K ⁻¹	ΔH^* KJ mol ⁻¹	ΔG^* KJ mol ⁻¹	R^2	Ea KJ mol ⁻¹	A S ⁻¹	ΔS^* mol ⁻¹ K ⁻¹	ΔH^* KJ mol ⁻¹	ΔG^* KJ mol ⁻¹
Ni	1 st	0.99	99	5.83×10^9	-59.9	67	93	0.99	72	5.87×10^1	-252	40	99
	2 nd	0.97	187	3.12×10^9	-225	150	115	0.97	110	1.32×10^1	-263	73	124
	3 rd	0.98	536	3.93×10^6	-163	494	132	0.99	190	8.47×10^1	-247	148	139
	4 th	0.90	921	8.80×10^{11}	-249	855	283	0.90	535	3.39×10^2	-260	469	253
Cu	1 st	0.96	32	3.32×10^{11}	-25.5	29	81	0.95	19	1.66×10^2	-204	65	87
	2 nd	0.98	38	1.13×10^8	-235	75	139	0.98	74	8.02×10^1	-245	135	129
	3 rd	0.99	178	5.50×10^6	-138	172	272	0.99	130	8.01×10^8	-83.4	124	184
Zn	1 st	0.94	153	1.02×10^{10}	-57	11	93	0.94	101	7.98×10^1	-256	6	125
	2 nd	0.91	311	1.98×10^8	-237	26	167	0.90	172	1.95×10^1	-252	12	162
	3 rd	0.90	567	8.39×10^2	-205	50	199	0.90	279	6.63×10^1	-239	21	195

Molecular modeling

Density functional theory (DFT) calculations for ligand and its metal complexes were carried out at B3LYP using Gaussian 09 quantum mechanical

(QM) calculations. The bond lengths, bond angles and geometrical structures (Fig. 10, 11) are in agreement with the thermal fragmentation (Table 6, 7).

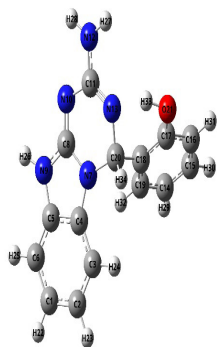


Fig. 10. Optimized structure of ligand and its numbering system.

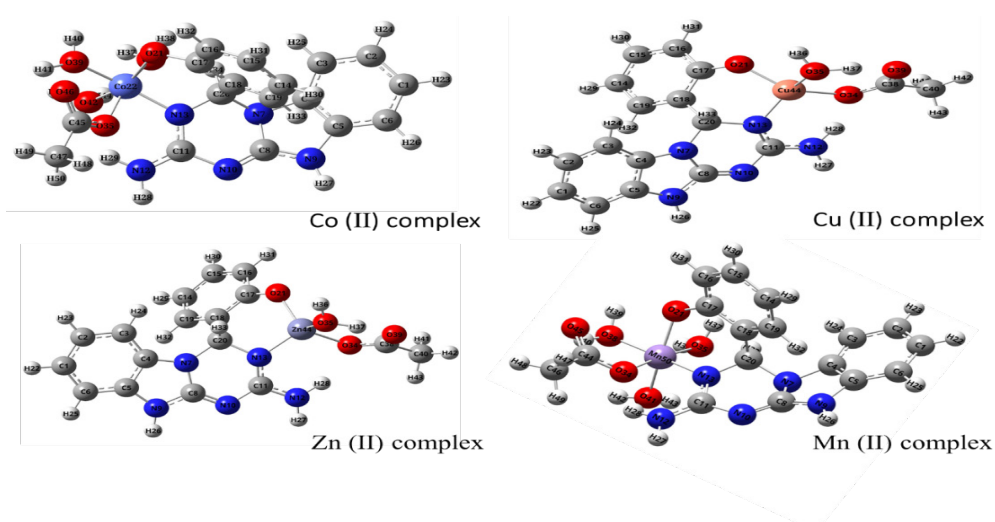


Fig. 11. Optimized structures of complexes and its numbering system.

TABLE 6. Optimized Structure Parameters of Ligand.

Structure parameters	B3LYP/3-21G*
rav(C-C) _{benzene ring}	1.399
rav(C-H) _{benzene ring}	1.083
<av(C-C-C) _{benzene ring}	120.0
rav(C-N)	1.416
rav(C=N)	1.306
r(C-O)	1.369
r(O-H)	1.045
E in Hartree	-923.31679 Hartree

Anticancer activity of Ligand and its Ni(II), Cu(II) and Zn(II) complexes

It is well known that the substance appears effective and exhibits cytotoxic activity when it is able to inhibit growth of cancer cells at low concentrations. Data compiled in Table 8 showed that ligand and its Cu(II) complex exhibited the highest cytotoxic activity against HEP-G2 with IC₅₀ value (43.9 and 3.5 µg/ml) which is comparable to that of the standard reference; Cisplatin (Table 8). This because of lower concentrations of the ligand and this complex required to decrease viability of these cancer cells. It was found that concentrations of the metal complex required to inhibit growth of cancer cells are convergent. This was in accordance with who reported that the metal complexes possess

higher cytotoxic activity against the selected human cancer cells[57]. The antitumor activity of metal complexes have more than one potential mechanism such as copper complexes where its activity could be related to transport of copper II ions into the cell [58]. The submission of copper II ions is carried out by specific copper transporters in the Cu (I) form. The presence of natural system for copper transportation enable us to cancel the using of exogenous drug carrier which is pivotal from clinical point of view. Thus, the interaction of metal complexes with proteins or nucleic acid determines the cellular effects of metal complexes activity. Considering metal complexes activity not only the interactions with DNA but also with proteins should be analyzed as the targeted molecules in antitumor mechanisms.

TABLE 7. Optimized Structure Parameters of Mn (II), Co (II), Cu (II) and Zn (II) complexes.

Structure parameters	Co(II) complex ^b	Zn(II) complex ^b	Mn(II) complex ^b	Cu(II) complex ^b
$r_{av}(C-C)_{\text{benzene ring}}$	1.399	1.401	1.399	1.400
$\langle r_{av}(C-C-C)_{\text{benzene ring}} \rangle$	119.9	119.9	120.0	120.0
$r_{av}(C-O)$	1.380	1.345	1.374	1.345
$r_{av}(C-N)$	1.408	1.417	1.412	1.411
$r_{av}(C=N)$	1.320	1.318	1.316	1.320
$r(M-N)_{\text{Ligand}}^a$	1.915	1.881	2.104	1.857
$r(M-O)_{\text{Ligand}}^a$	1.970	1.848	2.169	1.823
$r(M-O)_{\text{water}}^a$	1.963	1.902	2.456	1.886
$r(M-O)_{\text{Acetate}}^a$	1.929	1.910	2.062	1.896
E in Hartree	-2754.351184	-2996.948901	-2523.736336	-2858.729940

a) M = Co, Zn, Mn or Cu

b) DFT calculations were carried out at B3LYP/3-21G*

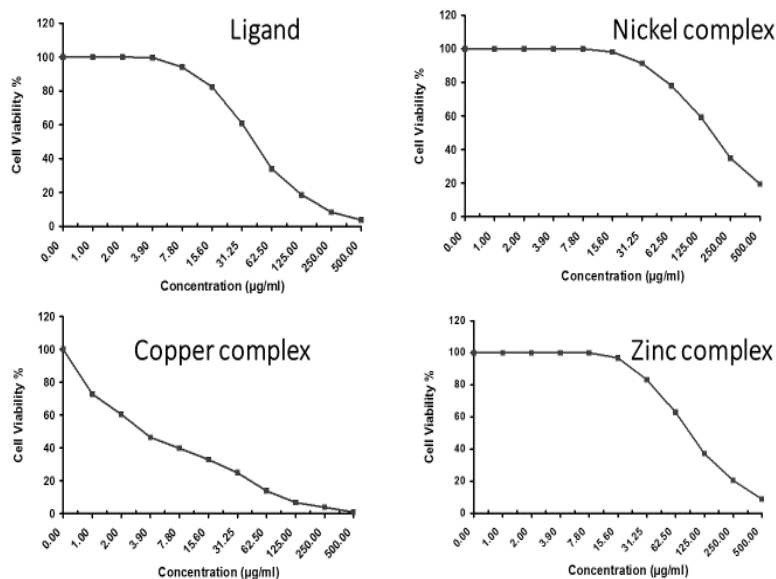


Fig. 12. Anticancer activity of Ligand and its Ni(II), Cu(II) and Zn(II) complexes.

TABLE 8. In vitro anticancer activity of ligand and nickel, copper and zinc complexes against HEP-G2 cell line.

Sample	Cisplatin	Ligand	Ni(II) complex	Cu(II) complex	Zn(II) complex
IC50 (µg/ml)	4.3	43.9	172	3.5	93.9

IC 50 = inhibition concentration 50%.

Conclusion

The novel ligand was obtained from cyclocondensation of 2-Guanidinobenzimidazole and Salicylaldehyde which acted as bidentate ligand and coordinated through the azomethine-N and hydroxy-O to the metal ions; Mn (II), Co (II), Ni (II), Cu (II) and Zn (II) forming novel complexes. The thermal dehydration and decomposition of Ni (II), Cu (II) and Zn (II) complexes show dehydration of water, and elimination of acetate then organic content and metal oxide remained as a residue. Although concentrations of the ligand and its Ni (II), Cu (II) and Zn (II) metal complexes required to inhibit growth of HEPG2 are in convergent, the Cu (II) complex exhibited the highest cytotoxic activity.

References

- Heras B.L., Amesty Á., Estévez-Braun A. and Hortelano S., Metal Complexes of Natural Product Like-compounds with Antitumor Activity. *Anti-Cancer Agents in Medicinal*, **19**(1), 48-65 (2019)
- a) Brandão P., Guieu S., Correia-Branco A., Silva C. and Martel F., Development of novel Cu (I) compounds with vitamin B1 derivative and their potential application as anticancer drugs. *Inorganica Chimica Acta*, **487**287-294 (2019).
b) Al-Wasidi, A.S., Naglah, A.M., Refat, M.S., El-Megharbel, S.M., Kalmouch, A., Moustafa, G.O. Synthesis, spectroscopic characterization and antimicrobial studies of Mn(II), Co(II), Ni(II), Cr(III) and Fe(III) melatonin drug complexes. *Egypt. J. Chem.*, **63** (4), in press, (2020).
- Abdel-Rahman L.H., Abu-Dief A.M., El-Khatib R.M. and Abdel-Fatah S.M., Sonochemical synthesis, DNA binding, antimicrobial evaluation and in vitro anticancer activity of three new nano-sized Cu (II), Co (II) and Ni (II) chelates based on tri-dentate NOO imine ligands as precursors for metal oxides. *Journal of Photochemistry and Photobiology B: Biology*, **162**298-308 (2016)
- Chen C.H., Huang W.S., Lai M.Y., Tsao W.C., Lin J.T., Wu Y.H., Ke T.H., Chen L.Y. and Wu C.C., Versatile, Benzimidazole/Amine-Based Ambipolar Compounds for Electroluminescent Applications: Single-Layer, Blue, Fluorescent OLEDs, Hosts for Single-Layer, Phosphorescent OLEDs. *Advanced Functional Materials*, **19**(16), 2661-2670 (2009)
- Patil S.A. and Patil R., Medicinal applications of (benz) imidazole- and indole-based macrocycles. *Chemical biology & drug design*, **89**(4), 639-649 (2017)
- Kim S.-K., Kim T.-H., Jung J.-W. and Lee J.-C., Polybenzimidazole containing benzimidazole side groups for high-temperature fuel cell applications. *Polymer*, **50**(15), 3495-3502 (2009)
- Chen D., Song H.Y., Sun E.T., Yu N. and Zou YUS patent 7,781,595 B2 (2010)
- Li Y.F., Wang G.F., Luo Y., Huang W.G., Tang W., Feng C.L., Shi L.P., Ren Y.D., Zuo J.P. and Lu W., Identification of 1-isopropylsulfonyl-2-amine benzimidazoles as a new class of inhibitors of hepatitis B virus. *European journal of medicinal chemistry*, **42**, 1358-1364 (2007)
- Al-Jorani K.R., Atia A.J.K., Lafta S.J., Al-Bayti R.I., Kadhém S.A. and Baqer S.M., Antibacterial Activity of New Benzimidazole Moiety Synthesis via Acid chloride and Related Heterocyclic Chalcones. *Journal of Pharmaceutical Sciences and Research*, **11**(4), 1195-1203 (2019)
- <http://nopr.niscair.res.in/handle/123456789/10085> Gowda J., Khadar A., Kalluraya B. and Kumari N.S., Microwave assisted synthesis of 1, 3, 4-oxadiazoles carrying benzimidazole moiety and their antimicrobial properties. (2010)
- Shi Y., Jiang K., Zheng R., Fu J., Yan L., Gu Q., Zhang Y. and Lin F., Design, Microwave-Assisted Synthesis and invitro Antibacterial and Antifungal Activity of 2, 5-Disubstituted Benzimidazole. *Chemistry & biodiversity*, **16**(3), e1800510 (2019)
- Villa P., Arumugam N., Almansour A.I., Kumar R.S., Mahalingam S., Maruoka K. and Thangamani S., Benzimidazole tethered pyrrolo [3, 4-b] quinoline with broad-spectrum activity against fungal pathogens. *Bioorganic & medicinal chemistry letters*, **29**(5), 729-733 (2019)

13. Wang X.J., Xi M.Y., Fu J.H., Zhang F.R., Cheng G.F. and You Q.D., Synthesis, biological evaluation and SAR studies of benzimidazole derivatives as H1-antihistamine agents. *Chinese Chemical Letters*, **23**(6), 707-710 (2012)
14. Lavrador-Erb K., Ravula S.B., Yu J., Zamani-Kord S., Moree W.J., Petroski R.E., Wen J., Malany S., Hoare S.R. and Madan A., The discovery and structure-activity relationships of 2-(piperidin-3-yl)-1H-benzimidazoles as selective, CNS penetrating H1-antihistamines for insomnia. *Bioorganic & medicinal chemistry letters*, **20**(9), 2916-2919 (2010)
15. Cuberes-Altisent M.R., Frigola-Constansa J. and Pares-Corominas J., US patent 5,182,280 (1993).
16. Jain P., Sharma P.K., Rajak H., Pawar R.S., Patil U.K. and Singour P.K., Design, synthesis and biological evaluation of some novel benzimidazole derivatives for their potential anticonvulsant activity. *Archives of pharmacal research*, **33**(7), 971-980 (2010)
17. Sahoo B.M., Banik B.K., Rao N.S. and Raju B., Microwave Assisted Green Synthesis of Benzimidazole Derivatives and Evaluation of Their Anticonvulsant Activity. *Current Microwave Chemistry*, **6**(1), 23-29 (2019)
18. Ibrahim H.S., Albakri M.E., Mahmoud W.R., Allam H.A., Reda A.M. and Abdel-Aziz H.A., Synthesis and biological evaluation of some novel thiobenzimidazole derivatives as anti-renal cancer agents through inhibition of c-MET kinase. *Bioorganic chemistry*, **85**337-348 (2019)
19. Vemana H.P., Barasa L., Surubhotla N., Kong J., Ha S.S., Palaguachi C., Croft J.L., Yoganathan S. and Dukhande V.V., Benzimidazole scaffolds as potential anticancer agents: Synthesis and Biological evaluation. *The FASEB Journal*, **33**646 (2019)
20. Akhtar M.J., Yar M.S., Sharma V., Khan A.A., Ali Z., Haider M.R. and Pathak A., Recent Progress of Benzimidazole Hybrids for Anticancer Potential. *Current Medicinal Chemistry*, (2020)
21. Rashid M., Husain A., Mishra R., Karim S., Khan S., Ahmad M., Al-Wabel N., Husain A., Ahmad A. and Khan S.A., Design and synthesis of benzimidazoles containing substituted oxadiazole, thiadiazole and triazolo-thiadiazines as a source of new anticancer agents. *Arabian Journal of Chemistry*, **12**(8), 3202-3224 (2019)
22. Kath R., Blumenstengel K., Fricke H. and Höffken K., Bendamustine monotherapy in advanced and refractory chronic lymphocytic leukemia. *Journal of cancer research and clinical oncology*, **127**(1), 48-54 (2001)
23. Renhowe P.A., Pecchi S., Shafer C.M., Machajewski T.D., Jazan E.M., Taylor C., Antonios-McCrea W., McBride C.M., Frazier K. and Wiesmann M., Design, structure-activity relationships and in vivo characterization of 4-Amino-3-benzimidazol-2-ylhydroquinolin-2-ones: a novel class of receptor tyrosine kinase inhibitors. *Journal of medicinal chemistry*, **52**(2), 278-292 (2009)
24. Trudel S., Li Z.H., Wei E., Wiesmann M., Chang H., Chen C., Reece D., Heise C. and Stewart A.K., CHIR-258, a novel, multitargeted tyrosine kinase inhibitor for the potential treatment of t (4; 14) multiple myeloma. *Blood*, **105**(7), 2941-2948 (2005)
25. Joensuu H., Blay J.-Y., Comandone A., Martin-Broto J., Fumagalli E., Grignani G., Del Muro X.G., Adenis A., Valverde C. and Pousa A.L., Dovitinib in patients with gastrointestinal stromal tumour refractory and/or intolerant to imatinib. *British journal of cancer*, **117**(9), 1278-1285 (2017)
26. Hammond L.A., Davidson K., Lawrence R., Camden J.B., Von Hoff D.D., Weitman S. and Izbicka E., Exploring the mechanisms of action of FB642 at the cellular level. *Journal of cancer research and clinical oncology*, **127**(5), 301-313 (2001)
27. Hao D., Rizzo J.D., Stringer S., Moore R.V., Marty J., Dexter D.L., Mangold G.L., Camden J.B., Von Hoff D.D. and Weitman S.D., Preclinical antitumor activity and pharmacokinetics of methyl-2-benzimidazolecarbamate (FB642). *Investigational new drugs*, **20**(3), 261-270 (2002)
28. Shrivastava N., Naim M.J., Alam M.J., Nawaz F., Ahmed S. and Alam O., Benzimidazole scaffold as anticancer agent: synthetic approaches and structure-activity relationship. *Archiv der Pharmazie*, **350**(6), e201700040 (2017)
29. Markman M., Blessing J.A., Moore D., Ball H. and Lentz S.S., Altretamine (hexamethylmelamine) in platinum-resistant and platinum-refractory ovarian cancer: a Gynecologic Oncology Group phase II trial. *Gynecologic oncology*, **69**(3), 226-229 (1998)
30. Rothenberg M.L., Liu P., Wilczynski S., Hannigan E.V., Weiner S.A., Weiss G.R., Hunter V.J., Chapman J.A., Tiersten A. and Kohler P.C., Phase
Egypt. J. Chem. **64**, No. 1 (2021)

- II trial of oral altretamine for consolidation of clinical complete remission in women with stage III epithelial ovarian cancer: a Southwest Oncology Group trial (SWOG-9326). *Gynecologic oncology*, **82**(2), 317-322 (2001)
31. Deepa P., Kolandaivel P. and Senthilkumar K., Theoretical investigation of interaction between psoralen and altretamine with stacked DNA base pairs. *Materials Science and Engineering: C*, **32**(3), 423-431 (2012)
32. Kong D. and Yamori T., Advances in development of phosphatidylinositol 3-kinase inhibitors. *Current medicinal chemistry*, **16**(22), 2839-2854 (2009)
33. Rania M., Mohamed A. and Hassan M., Design, Synthesis and Molecular Modeling of New 1, 3, 5-Triazine Derivatives as Anticancer Agents. *Der Pharma Chemica*, **11**(5), 7-14
34. Younis A., Hassan A.M., Mady M.F., El-Haddad A.F. and Fayad M., Utilization of Microwave Irradiation and Conventional Methods on Synthesis of Novel Pyridine Derivatives of Expected Anticancer Activity. *Journal of Chemical and Pharmaceutical Research*, **8**(9), 193-202 (2016)
35. Kateb A., Saleh T., Ali M., Elhaddad A. and El-Dosoky A., Microwave mediated facile synthesis of some novel pyrazole, pyrimidine, pyrazolo [1, 5-a] pyrimidine, triazolo [1, 5-a] pyrimidine and pyrimido [1, 2-a] benzimidazole derivatives under solvent less condition. *Nat Sci*, **10**(11), 77-86 (2012)
36. Younis A., Hassan A.M., Mady M.F., F. E.-H.A., A. Y.F. and Fayad M., Microwave-Assisted One-Pot Synthesis of Novel Polyarylpyrrole Derivatives of Expected Anticancer Activity. *Der Pharma Chemica*, **9**(3), 33-44 (2017)
37. a) Younis A., Fathy U., El-Kateb A.A. and Awad H.M., Ultrasonic assisted synthesis of novel anticancer chalcones using water as green solvent. *Der Pharma Chemica*, **8**(17), 129-136 (2016)
- b) Moustafa, G.O., Younis, A., Al-Yousef, S.A., Mahmoud, S.Y. Design, synthesis of novel cyclic pentapeptide derivatives based on 1, 2- benzenedicarbonyl chloride with expected anticancer activity., *J. Comput. Theor. Nanosci.* **16** (5-6), 1733-1739 (2019).
38. Fathy U., Younis A. and M. H.A., Ultrasonic assisted synthesis, anticancer and antioxidant activity of some novel pyrazolo[3,4-b]pyridine derivatives. *Journal of Chemical and Pharmaceutical Research*, **7**(9), 4-12 (2015)
39. Hassan A. M., Heikal B.H., Younis A., Bedair M.a.E.-M. and Mohamed M.M.A., Synthesis of Some Triazole Schiff Base Derivatives and Their Metal Complexes under Microwave Irradiation and Evaluation of Their Corrosion Inhibition and Biological Activity. *Egyptian Journal of Chemistry*, **62**(9), 1603-1624 (2019).
40. Younis A. and Awad G., Utilization of Ultrasonic as an Approach of Green Chemistry for Synthesis of Hydrazones and Bishydrazones as Potential Antimicrobial Agents. *Egyptian Journal of Chemistry*, **63**(2), 599-610 (2020).
41. El-Kateb A., Abd El-Rahman N., Saleh T., Ali M.H., El-Dosoky A. and Ghada E., Awad Microwave assisted 1, 3-Dipolar Cycloaddition Reactions of Some Nitrilimines and Nitrile Oxide to E-1-(4-(1-(4-aminophenyl) ethylideneamino) phenyl)-3-(dimethylamino) prop-2-ene-1-one under solventless conditions. *Journal of Applied Sciences Research*, **8**(7), 3393-3405 (2012).
42. El Alfy H., Hassan A. M., Khattab E.S.A. and Heikal B.H., Synthesis, Characterization and Biological Evaluation Studies of 4-((3-Formyl-4-hydroxyphenyl) diazanyl)-N-(4-methyloxazol-2-yl) Benzene Sulfonamide with Cu (II), Ni (II), Zn (II) and Ag (I) Using a Microwave Irradiation. *Egyptian Journal of Chemistry*, **61**(4), 569-580 (2018).
43. Hassan A. H., Heikal B.H., Said A.O., Aboulthana W.M. and Abdelmoaz M.A., Comparative study for synthesis of novel Mn (II), Co (II), Ni (II), Cu (II), Zn (II) and Zr (IV) complexes under conventional methods and microwave irradiation and evaluation of their antimicrobial and Anticancer activity. *Egyptian Journal of Chemistry*, in press(2020).
44. Hassan A.M., Heikal B.H., Soliman O., Abdalla K. and Abo El-Ata W., Microwave Irradiation Synthesis and Breast Carcinoma of 6-ethoxy-2-(2-methoxy-benzylideneamino) benzothiazole and Its Metal Complexes. *Egyptian Journal of Chemistry*, **62**(3), 401-414 (2019).
45. Furniss B.S., *Vogel's textbook of practical organic chemistry*. Pearson Education India(1989).
46. Coats A.W. and Redfern J.J.N., Kinetic parameters from thermogravimetric data. **201**, 68-69, (1964).
47. Horowitz H.H. and Metzger G.J.a.C., A new analysis of thermogravimetric traces. **35**(10), 1464-1468 (1963).
48. King F., Acheson R. and Spensley P., 275. Benzimidazole analogues of paludrine. *Journal of the Chemical Society (Resumed)*, 1366-1371 (1948)
- Egypt.J.Chem.* **64**, No.1 (2021)

49. a) Bauer A., Kirby W., Sherris J.C. and Turck, turck, Turck M. Antibiotic susceptibility testing by a standardized single disk method. *American journal of clinical pathology*, **45**(4), 493 (1966).
- b) Kassem, A.F., Moustafa, G.O., Nossier, E.S., Khalaf, H.S., Mounier, M.M., Al-Yousef, S.A., Mahmoud, S.Y. *In vitro* anticancer potentiality and molecular modelling study of novel amino acid derivatives based on N1, N3-bis-(1-hydrazinyl-1-oxopropan-2-yl) isophthalamide. *J. Enzyme Inhib. Med. Chem.* **34**(1), 1247-1258 (2019).
50. a) Clinical and Laboratory Standard Institute. Performance Standards for Antimicrobial Disk Susceptibility Tests; Approved Standard N.E., Clsi Document M2-A9. Clinical and Laboratory Standards Institute, USA. 2006.
- b) Zayed E. M., El-Samahy, F. A., Mohamed G. G. Structural, spectroscopic, molecular docking, thermal and DFT studies on metal complexes of bidentate orthoquinone ligand. *Appl Organometal Chem.* **33** (2019).
51. Mosmann T., Rapid colorimetric assay for cellular growth and survival: application to proliferation and cytotoxicity assays. *Journal of immunological methods*, **65**(1-2), 55-63 (1983).
52. Lal K., Singh J. and Gupta S., Complexes of 5- chloro-2- hydroxy-4- methyl acetophenone oxime with palladium (II), copper (II), nickel (II), cobalt (II), vanadyl (II), iron (III), uranyl (II) and molybdenyl (II). *Journal of Inorganic and Nuclear Chemistry*, **40**(2), 359-361 (1978).
53. Hassan A.M., Wahba O.A., Naser A. and Eldin A.M., Microwave synthesis and spectroscopic studies of some complex compounds as pigments and their applications in paints. *Journal of Coatings Technology and Research*, **13**(3), 517-525 (2016).
54. Ejidike I.P. and Ajibade P.A., Synthesis, characterization, antioxidant, and antibacterial studies of some metal (II) complexes of tetradentate schiff base ligand:(4E)-4-[(2-(E)-[1-(2, 4-dihydroxyphenyl) ethylidene] aminoethyl) imino] pentan-2-one. *Bioinorganic chemistry and applications*, (2015).
55. Low M.L., *Synthesis, characterization and bioactivities of dithiocarbamate Schiff base ligands and their metal complexes*. 2014.
56. Kivelson D. and Neiman R., ESR studies on the bonding in copper complexes. *The Journal of Chemical Physics*, **35**(1), 149-155 (1961).
57. Qin J.-L., Shen W.-Y., Chen Z.-F., Zhao L.-F., Qin Q.-P., Yu Y.-C. and Liang H., Oxoaporphine metal complexes (Co II, Ni II, Zn II) with high antitumor activity by inducing mitochondria-mediated apoptosis and S-phase arrest in HepG2. *Scientific reports*, **74**, 6056, (2017).
58. Gałczyńska K., Ciepluch K., Madej Ł., Kurdziel K., Maciejewska B., Drulis-Kawa Z., Węgierek-Ciuk A., Lankoff A. and Arabski M., Selective cytotoxicity and antifungal properties of copper (II) and cobalt (II) complexes with imidazole-4-acetate anion or 1-allylimidazole. *Scientific reports*, **9**(1), 1-13 (2019).

تصميم و تشييد و دراسات حاسوبية (DFT) و الفاعلية البيولوجية لمتراكبات جديدة
تحتوى على مجموعة 1 و3 و5-ترايزينو[1 و2-]a بنزاميدازول باستخدام الميكروويف كوسيلة
للكيمياء الخضراء

على مصطفى على حسن ، باسم هيكل و حمدى خميس ، جمال عبد النعيم و عماد مرزوق و ميرال أحمد
عبد المعزو أحمد يونس*

استخدام أشعة الميكروويف كأحد وسائل الكيمياء الخضراء فى تحضير متراكبات جديدة من المنجنيز و الكوبلت و النيكل و النحاس و الخارصين تحتوى على مشتق ترايزينوبنزاميدازول و قد تم اثبات و دراسة التركيب البنائى للمترابط و المتراكبات الجديدة باستخدام التحاليل الطيفية المختلفة و تحليل طيف الكتلة و التحاليل العنصرية و غيرها و تم اختبار الفاعلية البيولوجية للمترابط و بعض المتراكبات الجديدة على الخلايا السرطانية للكبد و أظهرت النتائج ان متراكب النحاس له فاعلية أفضل من المترابط و باقى المتراكبات التى تم اختبارها.